Available online at www.sciencedirect.com
ScienceDirect
Ceramics International 38S (2012) S153–S157
CERAMICS INTERNATIONAL
www.elsevier.com/locate/ceramint

Phase analysis and microwave dielectric properties of $BaO–Nd_2O_3–5TiO_2$ composite ceramics using variable size TiO_2 reagents

Amanda L. Snashall [a], Lasse Norén [a], Yun Liu [a,*], Toru Yamashita [b], Frank Brink [c], Raymond L. Withers [a]

[a] *Research School of Chemistry, The Australian National University, ACT 0200, Australia*
[b] *Materials Development, Mesaplexx Pty Ltd, QLD 4113, Australia*
[c] *Centre for Advanced Microscopy, The Australian National University, ACT 0200, Australia*

Available online 30 April 2011

Abstract

There are significant inconsistencies in published literature surrounding the phase analysis and physical properties of ceramics with the nominal composition $BaO–Nd_2O_3–5TiO_2$ (BNT125). A careful phase analysis investigation of BNT125 ceramics using variable size TiO_2 reagents was therefore undertaken using XRD, FESEM and EPMA with corresponding dielectric properties characterised over 2–3 GHz. Three distinct phases were consistently formed: $Ba_{6-3x}Nd_{8+2x}Ti_{18}O_{54}$ ($x \sim 0.67$), $Ba_2Ti_9O_{20}$ and TiO_2. The use of nano-scale TiO_2 reagents significantly reduced porosity and improved the dielectric properties of the composite ceramics, while markedly reducing processing times. Structural and crystal chemical indications as to the origin of this system's physical properties are discussed, with these results providing new insights into optimisation paths for microwave dielectric materials of this type.

Keywords: A. Sintering; B. Composites; C. Dielectric properties; D. Titanates

1. Introduction

Dielectric electroceramics are fundamental building blocks for microwave telecommunications technology, *e.g.* as dielectric resonators in filters, phase shifters and dielectric resonator antennas [1]. Materials of composition $BaO–Nd_2O_3–5TiO_2$ (the nominal composition henceforth referred to as BNT125), first reported in 1981 [2], display excellent microwave dielectric properties [3]. Subsequent investigations revealed that ceramics with this average composition were not single phase, but rather consisted of multiple phases [4,5] with the majority phase belonging to the nearby $Ba_{6-3x}Nd_{8+2x}Ti_{18}O_{54}$ solid solution (BNT124ss). Nevertheless, recent publications [6,7] continue to report the formation of 'single phase BNT125'.

The composition, individual dielectric properties and grain size of each of the phases present in any composite ceramic material such as BNT125 directly influence its overall physical properties. Clarification of the actual phases present in BNT125 (when at equilibrium) is thus essential to understanding and tuning its physical characteristics. This work reinvestigates the morphology, phase composition and physical properties of BNT125 ceramics, in particular focussing on phase analysis and observation of property modifications induced through varying the size of the TiO_2 reagent.

2. Experimental

BNT125 electroceramics were synthesised via solid state reaction using $BaCO_3$ (>2 N, May and Baker), Nd_2O_3 (3N, Pi-KEM) and μ-TiO_2 (2 N, Sigma–Aldrich) or n-TiO_2 (4 N, PiKEM, 20 nm). Resultant samples are henceforth referred to as BNT125μ and BNT125n, respectively. All starting materials were thoroughly dried prior to weighing, with Nd_2O_3 undergoing a high temperature (1000 °C) treatment. Reagents were mixed in appropriate ratios, ball-milled for 12 h under ethanol (polyoxymethylene canisters, stabilised ZrO_2 balls), dried, sieved to a particle size <125 μm and calcined at 1100 °C for 4 h. BNT125μ powders underwent a second 12 h ball-milling/sieving/drying process. BNT125n powders did not require any

* Corresponding author. Tel.: +61 2 6125 1124; fax: +61 2 6125 0750.
E-mail address: yliu@rsc.anu.edu.au (Y. Liu).

0272-8842/$36.00
doi:10.1016/j.ceramint.2011.04.070

additional processing. Poly-vinyl alcohol was used as an organic binder, with individual samples sintered between 1225 and 1300 °C on platinum foil. The optimum sintering temperature was found to be 1250 °C with samples sintered for 4 h (BNT125μ4 and BNT125n4) and 60 h (BNT125μ60 and BNT125n60) at this temperature. Densification was determined through the Archimedes method.

Phase composition was first investigated via XRD (Siemens D-5000 and Guinier-Hägg, Cu radiation), with pure Si (Sietronics GD#1) used as an internal standard. A field emission scanning electron microscope (FESEM, Hitachi 4300SE/N) was used to characterise both morphology and phase distribution. Quantitative analyses were undertaken via electron probe microanalysis (EPMA) conducted using a JEOL JSM6400 (15 kV, 1 nA). NdP_5O_{14}, $BaSO_4$ and TiO_2 (rutile) were used as calibration standards for EPMA analyses.

A network analyser (Agilent E5062A) was used to characterise dielectric properties using the S_{11} reflectance model, based on the TE_{011} resonant mode. Q values were calculated using "QZERO for Windows" developed by Kajfez. The dielectric constant (ε_r) was obtained using a 3D finite element analysis (FEA) *eigenmode* solver. The temperature coefficient of resonant frequency (τ_f) was calculated via the relation $\tau_f = \Delta f/f\Delta T$ (ppm/°C).

3. Results and discussion

XRD patterns of synthesised BNT125 matched published BNT125 patterns, with the extracted lattice parameters also in good agreement as displayed in Table 1. Very weak additional lines arising from TiO_2-rutile were also observed suggesting a two-phase mixture of '$BaNd_2Ti_4O_{12}$' (tungsten bronze type $Ba_{6-3x}Nd_{8+2x}Ti_{18}O_{54}$ (BNT124ss), $x = 0.5$) and TiO_2, in accordance with previously published results [5]. Small but non-trivial reductions in the normalised cell volumes of the majority BNT124ss phase relative to the known unit cell volume of BNT124ss ($x = 0.5$) were observed. This implied a shift in composition of this solid solution phase towards a higher x value (higher lanthanide content), thereby necessitating the formation of a third, Ba-rich, phase in order to adhere to the nominal BNT125 composition. The good agreement between the unit cell parameters of the synthesised and reported BNT125 samples indicate that the latter also contained a majority BNT124 solid solution phase with $x > 0.5$ (necessitating a ternary phase composition, contrary to most previously published reports [3,5–8]).

Table 1
Unit cell parameters for the compounds "$BaNd_2Ti_4O_{12}$" (BNT124ss, $x = 0.5$) and "$BaNd_2Ti_5O_{14}$" (BNT125) reported in literature and from this study [+].

Type	a (Å)	b (Å)	c (Å)	V[a] (Å^3)
(BNT125) [3]	22.346(2)	12.201(1)	3.8404(3)	2094.12
(BNT125) [8]	12.1983(13)	22.347(3)	3.8403(6)	2093.70
(BNT124) [9]	22.343	12.213	7.696	2100.05
(BNT124) [10]	22.354(4)	12.211(2)	3.8512(7)	2102.46
(BNT124) [17]	22.3479(3)	7.6955(1)	12.2021(2)	2098.50
BNT125 μ4 [+]	22.3172(14)	12.1882(8)	7.6805(6)	2089.13
BNT125n4 [+]	22.3318(23)	12.1975(12)	7.6820(8)	2092.52

[a] In all cases the unit cell volume (V) has been standardised to reflect the setting given by Varfolomeev et al. [9] in order to improve comparability.

Irrespective of TiO_2 particle size or annealing time, our BNT125 samples always displayed a readily visible ternary phase nature as shown in Fig. 1(a). This effectively ruled out potential phase contributions from non-equilibrated samples. The resultant Ba^{2+} rich phase, previously reported [4] as $BaTi_4O_9$, was identified as $Ba_2Ti_9O_{20}$ via SEM–EPMA. Table 2 displays quantitative EPMA results, confirming the three phases constituent phases as (1) tungsten bronze type $Ba_{6-3x}Nd_{8+2x}Ti_{18}O_{54}$ ($x \sim 0.65$–0.70), (2) $Ba_2Ti_9O_{20}$ and (3) TiO_2. Fig. 1(b) displays a phase diagram, indicating the nominal BNT125 composition in addition to the three phases subsequently identified as forming the composite BNT125 material. Quantitative results for (3) TiO_2 were difficult to attain due to the small grain size, however, analyses at a reduced accelerating voltage (5 kV) indicated that this phase was indeed pure TiO_2, confirming the results obtained via XRD.

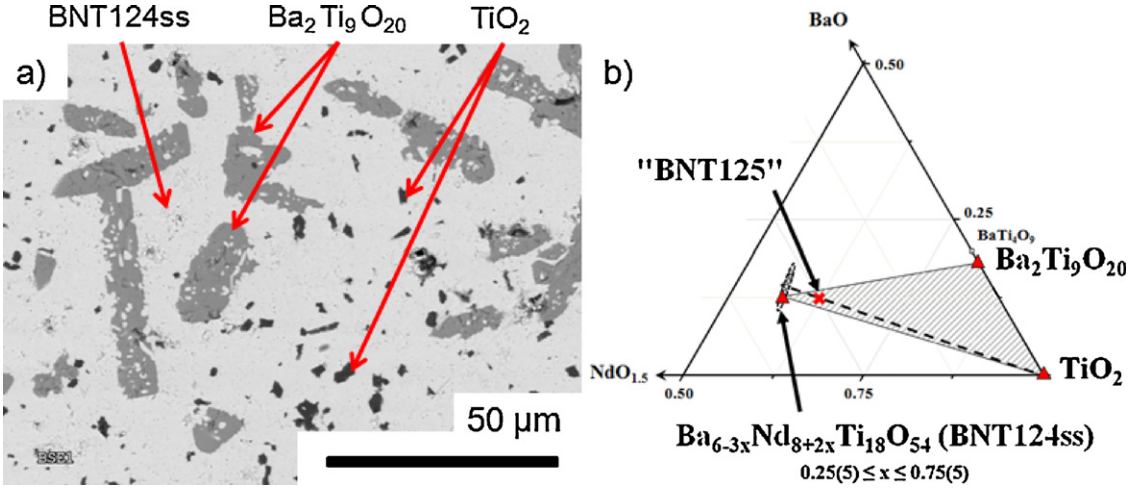

Fig. 1. (a) Back scattered electron image of BNT125n60 displaying tertiary phase nature and (b) a phase diagram displaying the position of the three compounds discovered (▲) and the nominal BNT125 composition (✖).

Table 2
Summarised EPMA analysis of BNT125 synthesised ceramics. Grain size inhibits quantitative measurement of phase (3), however, low accelerating voltage analyses indicate a TiO_2 composition.

Composition	BNT125μ4	BNT125μ60	BNT125n4	BNT125n60
(1) $Ba_{6-3x}Nd_{8+2x}Ti_{18}O_{54}$	x (Ba) = 0.70(5)	x (Ba) = 0.72(3)	x (Ba) = 0.64(3)	x (Ba) = 0.66(4)
	x (Nd) = 0.7(15)	x (Nd) = 0.71(2)	x (Nd) = 0.63(8)	x (Nd) = 0.69(3)
(2) $BaTi_{4.5}O_{10}$ ($Ba_2Ti_9O_{20}$)	Ba: 0.99(2)	Ba: 1.00(4)	Ba: 1.02(2)	Ba: 1.00(1)
	Nd: 0.05(5)	Nd: 0.02(1)	Nd: 0.01(2)	Nd: 0.03(2)
	Ti: 4.47(4)	Ti: 4.49(1)	Ti: 4.48(1)	Ti: 4.48(1)

The composition range of the $Ba_{6-3x}Nd_{8+2x}Ti_{18}O_{54}$ solid solution (BNT124ss) phase is reported to lie between $0.25(5) < x < 0.75(5)$ [9]. It has been reported [10] that this range is dependent on both sintering temperature and quenching speed leading to the conclusion that equilibrium is difficult to achieve. This tungsten bronze type structure is composed of corner shared TiO_6-octahedra forming three distinct sites for cation insertion: the 12-coordinated '*R*' site preferentially occupied by Nd^{3+} ions, the 15-coordinated '*P*'-site predominantly accommodating Ba^{2+} ions, and the 9-coordinated '*T*'-site that is invariably vacant due to its restrictive size [11]. Ba^{2+} can partially substitute for Nd^{3+} in the smaller '*R*'-site forming the lower limit of the solid solution ($x = 0.25(5)$), while Nd^{3+} partial substitution for Ba^{2+} in the '*P*'-site defines the upper limit ($x = 0.75(5)$). At $x = 0.67$ the structure is reported to be in its least strained state due to complete segregation of the Ln^{3+} ions and Ba^{2+} ions into the '*R*' and '*P*'-sites, respectively [11,12].

BNT125μ samples displayed an average $x \geq 0.7$ while BNT125n samples displayed an average $x \geq 0.64$, all corresponding to the Nd^{3+} rich end of the $Ba_{6-3x}Nd_{8+2x}Ti_{18}O_{54}$ O_{54} solid solution. The larger standard deviation in x displayed by BNT125μ4 suggested that this sample had not reached equilibrium, with prolonged annealing (BNT125μ60) resulting in much higher compositional uniformity. BNT125n4 displays a much lower standard deviation than the BNT125μ4 sample, indicating that equilibrium is achieved much faster through the use of n-TiO_2. Through prolonged annealing, BNT125n displayed enhanced diffusion of Ba^{2+} and Nd^{3+} ions, resulting in a reduction in compositional variation and a movement towards an equilibrium position of $x \sim 0.67$.

Bond valence sum (BVS) and global instability index calculations (GII) are used to calculate ''the apparent valence'' of ions and to indicate the overall stability of a structure [13]. As shown in Table 3, calculated GII's for the $Ba_{6-3x}Nd_{8+2x}$-$Ti_{18}O_{54}$ structure indicate that for $0.67 \leq x \leq 0.71$ BVS are closer to the ideal values. This result corroborates previous findings [11] showing that the $x = 0.67$ composition results in the lowest possible strain. Improbable GII's for $x < 0.67$ can be primarily attributed to enforced Ba^{2+} placement on '*R*'-sites, resulting in an apparent valance of ~3.8–4.5 for these ions. For values of $x > 0.71$ the strain imposed on the structure through '*R*'-site vacancies and Nd^{3+} under-bonding form the upper limit of x. These results provide a clear crystal chemical explanation as to why the majority BNT124ss phase of BNT125 composite ceramics deviates from $x = 0.5$, thereby forcing the ternary phase nature of BNT125.

Surface morphology was investigated via SEM imaging to observe densification behaviour, as porosity significantly degrades microwave dielectric performance. Fig. 2(a) shows the considerable porosity and poor grain growth of BNT125μ4. As can be seen in Fig. 2, BNT125n60 shows the best densification, with a larger grain size than BNT125n4 and enhanced grain size uniformity when compared to BNT125μ60. As shown in Table 4, BNT125n4 displays a >14% increase in density compared to BNT125μ60, demonstrating that the use of n-TiO_2 provides significant improvements in densification, while substantially reducing processing and annealing time. Only trivial changes in density were observed between BNT125n4 and BNT125n60, indicating that sintering was effectively completed after only 4 h.

The dielectric properties of the samples varied significantly with changes in TiO_2 reagent grain size and annealing times as detailed in Table 4. BNT125n samples displayed substantially enhanced ε_r when compared to BNT125μ4 and BNT125μ60 (~30% and ~25% increase, respectively) corresponding to improved densification. Prolonged annealing of BNT125μ samples was also observed to improve Q, attributed to a decrease in Ba^{2+} over-bonding resultant from movement of the dominant phase towards the lower GII $0.67 \leq x \leq 0.71$ compositions. Prolonged annealing of BNT125n did not alter ε_r, however, slight increases in both Q and τ_f were observed. The slightly higher Q exhibited by BNT125μ60 when compared to BNT125n60 can be attributed to a relative change

Table 3
Global instability index (GII) values calculated from bond valance sum (BVS) calculations for $Ba_{6-3x}Ln_{8+2x}Ti_{18}O_{54}$ (Ln = Sm [15], Nd [16,17]) structures over various '*x*' parameter values.

	$x = 0.30$	$x = 0.50$	$x = 0.67$	$x = 0.71$	$x = 0.75$
Ln = Nd (GII (v.u.))	0.63	0.59			0.37
Ln = Sm (GII (v.u.))		0.60	0.17	0.16	

Table 4
Properties of 1250 °C sintered BNT125 samples using μ-TiO_2 and n-TiO_2 precursor powders and various annealing times.

	BNT125μ4	BNT125μ60	BNT125n4	BNT125n60
Density (g/cm^3)	4.59	4.78	5.46	5.47
Qf	7906	8880	8584	8712
ε_r	61	63.5	79.5	79.5
τ_f (ppm/°C)	76	79	76	81

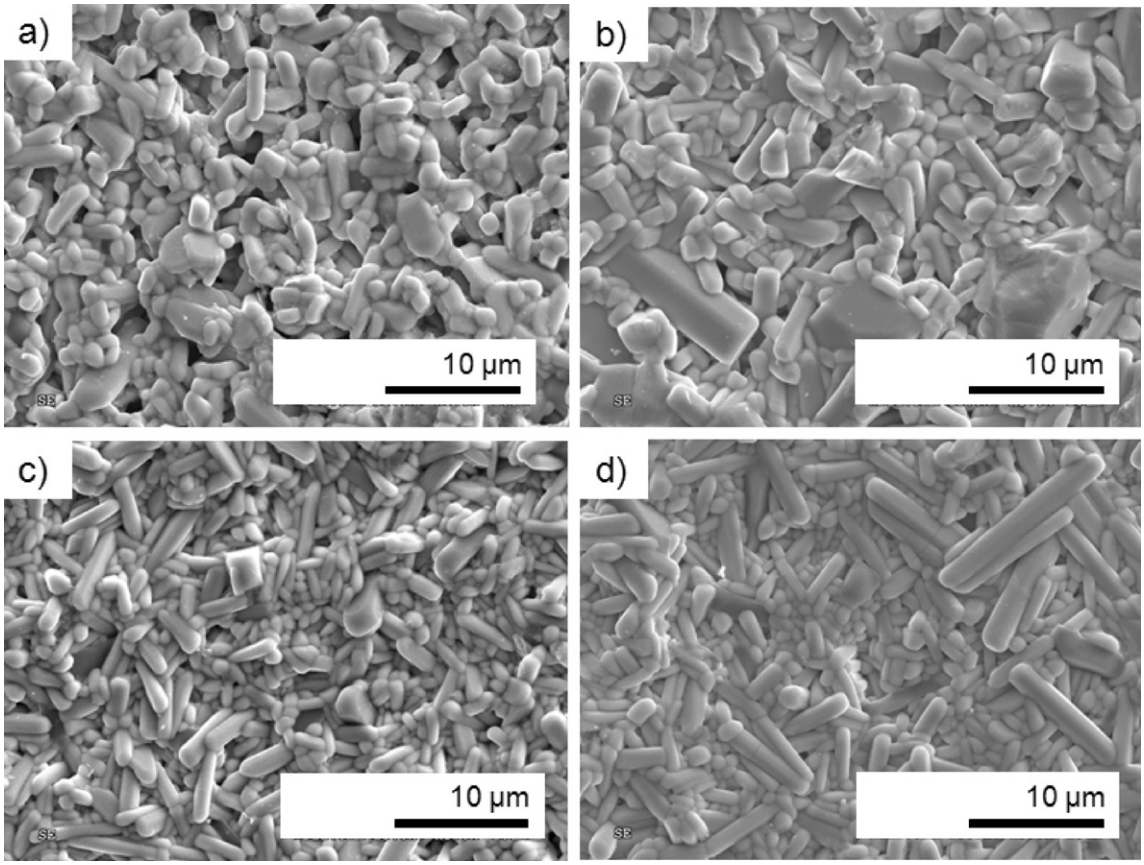

Fig. 2. Surface morphologies of BNT125 ceramics sintered at 1250 °C for various annealing times (a) BNT125 μ4, (b) BNT125n4, (c) BNT125μ60 and (d) BNT125n60.

in phase composition between the ternary phases. BNT125μ60's majority phase ($Ba_{6-3x}Nd_{8+2x}Ti_{18}O_{54}$) is more deficient in Ba^{2+} when compared to BNT125n60 and as a result must contain a higher proportion of $Ba_2Ti_9O_{20}$. As $Ba_2Ti_9O_{20}$ has a significantly higher Q (Qf = 32,000) [14] than $Ba_{6-3x}Nd_{8+2x}Ti_{18}O_{54}$, the larger proportion of this phase within the BNT125μ60 composite results in the higher Qf values observed. The same observations are also valid for Qf improvements observed through prolonged annealing of BNT125n powders.

4. Conclusions

It was confirmed that under all synthesis conditions tested BNT125 did not produce a single-phase product, irrespective of annealing time or reagent particle size. BNT125 was instead found to form three distinct phases: $Ba_{6-3x}Nd_{8+2x}Ti_{18}O_{54}$ ($x = \sim 0.7$), $Ba_2Ti_9O_{20}$ and TiO_2 contrary to previous reports indicating single, binary or alternate ternary phase compositions. Through the use of a nano-particulate TiO_2 reagent it has been shown that significant reductions in processing and annealing times can be achieved in addition to the formation of dielectrically superior products. This provides new insight into optimisation paths for producing dielectrically superior composite materials of this type.

Acknowledgements

ALS, YL, TY and RLW thank the Australian Research Council for financial support in the form of ARC Linkage Grants. ALS particularly appreciates her Australian Postgraduate Award Industry scholarship.

References

[1] L. Nedelcu, M.I. Toacsan, M.G. Banciu, A. Ioachim, Dielectric resonators for microwave and millimeter wave applications, IEEE Semiconductor Conference 2 (2007) 275–278.
[2] D. Kolar, S. Gabarscek, B. Volavsek, H.S. Parker, R.S. Roth, Synthesis and crystal chemistry of $BaNd_2Ti_3O_{10}$, $BaNd_2Ti_5O_{14}$, and $Nd_4Ti_9O_{24}$, Journal of Solid State Chemistry 38 (1981) 158–164.
[3] Y.P Fu, C.W. Liu, C.H. Lin, C.K. Hsieh, Effect of TiO_2 ratio on BaO–Nd_2O_3–TiO_2 microwave ceramics, Ceramics International 31 (2005) 667–670.
[4] T. Jaakola, A. Uusimäki, R. Rautioaho, S. Leppävuori, Matrix phase in ceramics with composition near BaO–Nd_2O_3–5TiO_2, Journal of the American Ceramic Society 69 (1986) C234–C235.
[5] J. Takahashi, T. Ikegami, K. Kageyama, Occurrence of dielectric 1:1:4 compound in the ternary system BaO–Ln_2O_3–TiO_2 (Ln = La, Nd, and Sm): II. Reexamination of formation of isostructural ternary compounds in identical systems, Journal of the American Ceramic Society 74 (1991) 1873–1879.
[6] Y.N. Ko, D.S. Jung, J.M. Han, H.Y. Koo, M.J. Lee, Y.C. Kang, Characteristics of $BaNd_2Ti_5O_{14}$ powders directly prepared by high-temperature spray pyrolysis, Ceramics International 36 (2010) 63–68.

[7] Z. Fu, P.M. Vilarinho, A. Wu, A.I. Kingon, Textured microstructure and dielectric properties relationship of $BaNd_2Ti_5O_{14}$ thick films prepared by electrophoretic deposition, Advanced Functional Materials 19 (2009) 1071–1081.

[8] M.C. Morris, H.F. McMurdie, E.H. Evans, B. Paretzkin, H.S. Parker, N.P. Pyrros, C.R. Hubbard, Standard X-ray diffraction powder patterns – section 19 – data for 51 substances, National Bureau of Standards (United States) Monograph 25 (S19) (1982) 19.

[9] M.B. Varfolomeev, A.S. Mironov, V.S. Kostomarov, L.A. Golubtsova, T.A. Zolotova, Preparation and homogeneity region of barium lanthanide titanium oxide ($Ba_{6-x}Ln_{8+2x/3}Ti_{18}O_{54}$), Russian Journal of Inorganic Chemistry (English Translation) 33 (1988) 607–609.

[10] K.M. Cruickshank, X. Jing, G. Wood, E.E. Lachowski, A.R. West, Barium neodymium titanate electroceramics: phase equilibria studies of $Ba_{6-3x}Nd_{8+2x}Ti_{18}O_{54}$ solid solution, Journal of the American Ceramic Society 79 (1996) 1605–1610.

[11] H. Ohsato, Science of tungsten bronze-type like $Ba_{6-3x}R_{8+2x}Ti_{18}O_{54}$ (R = rare earth) microwave dielectric solid solutions, Journal of the European Ceramic Society 21 (2001) 2703–2711.

[12] H. Ohsato, M. Imaeda, The quality factor of the microwave dielectric materials based on the crystal structure – as an example: the $Ba_{6-3x}R_{8+2x}Ti_{18}O_{54}$ (R = rare earth) solid solutions, Materials Chemistry and Physics 79 (2003) 208–212.

[13] SoftBV v0.96. http://www.softbv.net/index.html (accessed 7/1/2011).

[14] J.K. Plourde, D.F. Linn, H.M. O'Bryan Jr., J. Thomson Jr., $Ba_2Ti_9O_{20}$ as a microwave dielectric resonator, Journal of the American Ceramic Society 58 (1975) 418–420.

[15] H. Okudera, H. Nakamura, H. Toraya, H. Ohsato, Tungsten bronze-type solid solutions $Ba_{6-3x}Sm_{8+2x}Ti_{18}O_{54}$ (x = 0.3. 0. 5, 0. 67, 0. 71) with superstructure, Journal of Solid State Chemistry 142 (1999) 336–343.

[16] L. Zhang, X.M. Chen, N. Qin, X.Q. Liu, Upper limit of x in $Ba_{6-3x}Nd_{8+2x}Ti_{18}O_{54}$ new tungsten bronze solid solution, Journal of the European Ceramic Society 27 (2007) 3011–3016.

[17] C.C. Tang, M.A. Roberts, F. Azough, C. Leach, R. Freer, Synchrotron X-ray diffraction study of $Ba_{4.5}Nd_9Ti_{18}O_{54}$ microwave dielectric ceramics at 10–295 K, Journal of Materials Research 17 (2002) 675–682.